Dust formation around AGB and SAGB stars: a trend with metallicity?

P. Ventura,[1] M. Di Criscienzo,[1] R. Schneider,[1] R. Carini,[1,2] R. Valiante,[1]
F. D'Antona,[1] S. Gallerani,[1] R. Maiolino,[3] A. Tornambé[1]

[1]*INAF – Osservatorio Astronomico di Roma, Via Frascati 33, 00040, Monte Porzio Catone (RM), Italy*
[2]*Dipartimento di Fisica, Università di Roma "La Sapienza", P.le Aldo Moro 5, 00143, Roma, Italy*
[3]*Cavendish Laboratory, University of Cambridge, 19 J.J. Thomson Ave., Cambridge CB3 OHE, UK*

ABSTRACT

We calculate the dust formed around AGB and SAGB stars of metallicity Z=0.008 by following the evolution of models with masses in the range $1 M_\odot \leqslant M \leqslant 8 M_\odot$ through the thermal pulses phase, and assuming that dust forms via condensation of molecules within a wind expanding isotropically from the stellar surface. We find that, because of the strong Hot Bottom Burning (HBB) experienced, high mass models produce silicates, whereas lower mass objects are predicted to be surrounded by carbonaceous grains; the transition between the two regimes occurs at a threshold mass of $3.5 M_\odot$. These findings are consistent with the results presented in a previous investigation, for Z=0.001. However, in the present higher metallicity case, the production of silicates in the more massive stars continues for the whole AGB phase, because the HBB experienced is softer at Z=0.008 than at Z=0.001, thus the oxygen in the envelope, essential for the formation of water molecules, is never consumed completely. The total amount of dust formed for a given mass experiencing HBB increases with metallicity, because of the higher abundance of silicon, and the softer HBB, both factors favouring a higher rate of silicates production. This behaviour is not found in low mass stars, because the carbon enrichment of the stellar surface layers, due to repeated Third Drege Up episodes, is almost independent of the metallicity. Regarding cosmic dust enrichment by intermediate mass stars, we find that the cosmic yield at Z=0.008 is a factor ∼5 larger than at Z=0.001. In the lower metallicity case carbon dust dominates after ∼300 Myr, but at Z=0.008 the dust mass is dominated by silicates at all times, with a prompt enrichment occurring after ∼40 Myr, associated with the evolution of stars with masses $M \sim 7.5 - 8 M_\odot$. These conslusions are partly dependent on the assumptions concerning the two important macro–physics inputs needed to describe the AGB phase, and still unknowm from first principles: the treatment of convection, which determines the extent of the HBB experienced and of the Third Dredge–up following each thermal pulse, and mass loss, essential in fixing the time scale on which the stellar envelope is lost from the star.

Key words: Stars: abundances – Stars: AGB and post-AGB. ISM: abundances, dust

1 INTRODUCTION

A reliable estimate of the nature and the amount of dust produced by stars of intermediate mass ($1 M_\odot \leqslant M \leqslant 8 M_\odot$) proves essential for a number of scientific issues. These stars are believed to be the dominant stellar sources of dust in the present-day Universe and, contrary to previous claims, their contribution to dust enrichment can not be neglected even at redshift $z > 6$ (Valiante et al. 2009, 2011). While the formation of dust in the ejecta of core-collapse super-novae has received much attention, both on the theoretical

(Bianchi & Schneider 2007; Hirashita et al. 2008; Todini & Ferrara 2001) and observational side (Dunne et al. 2009; Morgan et al. 2003; Rho et al. 2008), models for the nucleation of dust grains in the atmospheres of intermediate mass stars have been computed either assuming synthetic stellar models (Ferrarotti & Gail 2001, 2002, 2006) or exploring a single value for the initial stellar metallicity (Ventura et al. 2012). In order to properly include their contribution in chemical evolution models with dust, the mass and composition of dust grains released by each star as a function of

its mass and metallicity need to be known. In addition, the corresponding size distribution function allows to compute the extinction properties associated with these grains, which is fundamental information required for correctly interpreting the optical-near infrared properties of high-z quasar and gamma ray burst spectra (Gallerani et al. 2010; Maiolino et al. 2004; Stratta et al. 2011).

Intermediate mass stars, after the end of the core–Helium burning phase, are nuclearly supported by a H–burning shell above the degenerate core, composed of carbon and oxygen (Iben 1975, 1976). He–burning occurs periodically in the helium–rich buffer, in conditions of thermal instability (Schwarzschild & Harm 1965, 1967); this motivates the term "Thermal Pulse" (TP) used to describe these episodes. Due to the position in the HR diagram, this evolutionary phase is known as Asymptotic Giant Branch (hereinafter AGB); AGB stars gradually loose all their envelope, ending their evolution as White Dwarfs (WD). During the AGB phase, characterized by strong mass loss, the conditions are most favourable for the condensation of gas molecules into dust.

The series of papers by the Heidelberg group (Gail & Sedlmayr 1999; Ferrarotti & Gail 2001, 2002, 2006; Zhukovska et al. 2008; Zhukovska & Gail 2009) set the framework to describe the dust formation process in the environment of AGBs. The scheme is based on a model of an expanding wind, whose thermodynamical structure is determined by the physical parameters of the central object, i.e. surface gravity, effective temperature, and the rate at which mass loss occurs.

In the first paper of this series (Ventura et al. 2012, hereinafter paper I), we made a step forward, by applying the wind modelling from Ferrarotti & Gail (2006) to AGB models calculated with a full integration of the whole stellar structure, more suitable than the synthetic technique to deal with phenomena based on the thermodynamical coupling between the internal, degenerate core, and the outer convective zone. The typical example is the Hot Bottom Burning (Renzini & Voli 1981), i.e. the series of proton–capture reactions at the bottom of the convective zone, once the temperature in that region reaches $T_{bce} \sim 40 - 50$ MK. The HBB phenomenon, active in models where the stellar mass exceeds a threshold value of $\sim 3 - 4$ M$_\odot$, is relevant for the production of elements as well as the physical properties of the star. As regarding the surface chemistry, the main effect of HBB is the depletion of the surface carbon, and possibly (when $T_{bce} > 80$ MK) oxygen, which prevents the formation of a C–star. The evolution of the star is also affected by HBB, because it is accompanied by a steep increase in the luminosity and mass loss of the star (Blöcker & Schöenberner 1991), so that the evolution becomes faster, and only a limited number of Thermal Pulses (TPs) is experienced (see, e.g., Ventura & D'Antona (2009)).

A strong HBB naturally limits the effects of the alternative mechanism that can modify the surface chemistry of AGBs, i.e. the Third Dredge–Up (TDU), which is the inward penetration of the envelope in the phases following the TP, when the surface convection can reach layers previously exposed to 3α nucleosynthesis (Iben 1975; Lattanzio 1986, 1989; Wood 1981). The main effect of the TDU is a great increase in the surface carbon, that eventually may become more abundant than oxygen, creating a C–star.

The kind of dust formed is extremely sensitive to which of the two afore mentioned mechanisms dominate the evolution of the surface chemistry of the star: repeated TDU episodes favour the formation of carbon–rich grains, whereas HBB destroys carbon, enabling the production of silicates.

In paper I, we showed that under HBB conditions the formation of carbon–rich dust is inhibited, and only silicates are produced. This introduces a dichotomy in the type of dust produced by AGBs: the more massive stars produce silicates, whereas lower-mass objects produce carbon dust. The analysis outlined interesting differences with the results by Ferrarotti & Gail (2006), that can all be understood on the basis of the different HBB experienced by the stars.

In this paper, we compare the results of paper I, that were limited to a single stellar metallicity ($Z = 0.001$), to AGB and Super-AGB (SAGB, stars of higher masses that evolve on a core made of Oxygen and Neon) stellar models with initial metallicity $Z = 0.008$. The main goal is to understand how the dust formed around AGBs and SAGBs changes with the initial chemical composition of the stars, and whether the basic difference between the type of dust formed around massive AGBs and lower–mass stars (producing, respectively, silicates and carbon–rich dust) persists. To this aim, we calculated a new set of AGB and SAGB models of metallicity $Z = 0.008$, and applied the same scheme used by Ferrarotti & Gail (2006) and in paper I to calculate the dust produced in their surroundings.

The paper is organized as follows. Section 2 describes the modelling of the stellar evolution and of the structure of the wind; the evolution properties of AGB and SAGB stars are discussed in Section 3; the results concerning the quantity and the type of dust produced are given in Section 4, whereas Section 5 deals with the uncertainties associated to the choices of the input macro–physics and of the optical constants of the silicates; finally, the results are discussed and commented in Section 6.

2   THE MODEL

Dust grains are assumed to form from condensation of gas molecules present in the expanding winds. The description of this process, and the determination of the kind and quantity of dust species formed, requires an accurate modelling of the evolution of the star along the AGB (or SAGB) phase, from which we obtain the temporal variation of mass, mass loss rate, luminosity, effective temperature, and the surface chemical composition: all this information is used to model the thermodynamical and chemical structure of the wind, hence to describe the dust formation process.

A word of caution in needed here. Mass loss during the AGB phase is here obtained by means of semi–empirical descriptions, that include some parameters, calibrated based on the comparison with the observations. More precisely, we assume a mass-loss rate and then compute the corresponding wind properties and the required degree of dust condensation. In reality, however, the mass loss is believed to be a consequence of dust formation, which makes such modeling approach seem somewhat circular. But we like to stress that this is the best one can do at present at a reasonable computational cost.

In what follows we provide a brief description of the

numerical scheme adopted; we refer to Ventura et al. (1998) and to paper I for further details.

2.1 Stellar evolution modelling

The stellar models presented in this work were calculated by means of the ATON stellar evolution code, in the version described in Ventura et al. (1998).

The extension of the convective regions was determined via the classic Schwartzschild criterium, stating that the convective instability is favoured by the condition $\nabla_{\rm rad} > \nabla_{\rm ad}$, where ∇ is the logarithmic gradient of temperature with respect to pressure. The temperature gradient within regions unstable to convective motions was determined by means of the Full Spectrum of Turbulence (hereinafter FST) model for turbulent convection (Canuto & Mazzitelli 1991). In the convective regions where the temperature is sufficiently large to allow the ignition of nuclear reactions, we follow the variation of the chemistry by coupling the convective motions with the process of nuclear burning, by means of a diffusive approach, according to the scheme by Cloutman & Eoll (1976). The velocities determined via the convection modelling are used to find the diffusion coefficients, and also to provide the extension of a possible extra–mixing zone, based on an exponential decay of velocities from the formal convective/radiative interface, determined on the basis of the Schwartzschild criterium: the scale for the decay of velocities is $l = \zeta H_p$, where ζ is the free parameter associated to the extension of the extra–mixed region. We assumed $\zeta = 0.02$ during the evolution before the beginning of the Thermal Pulses phase, in agreement with the calibration given in Ventura et al. (1998). For what concerns the AGB phase, we compare the results found ignoring any overshoot from the convective borders, with those obtained by assuming a tiny extra–mixing from the convective shells developed as a consequence of the ignition of the Thermal Pulse, with $\zeta = 0.001$.

Mass loss was modelled following Blöcker (1995), with the free parameter entering this recipe set to $\eta_R = 0.02$. The value for η_R was calibrated specifically for this range of masses and for this metallicity via a comparison between the observed and the predicted luminosity function of lithium rich sources and of carbon stars in the Large Magellanic Cloud (Ventura et al. 1999, 2000).

The OPAL radiative opacities (Iglesias & Rogers 1996) were used for temperatures above 10^4 K, whereas for smaller temperatures we used the AESOPUS tool described in Marigo & Aringer (2009). This choice allows to account for the increase in the opacity associated with the enrichment in the surface carbon, as a consequence of the TDU: this is particularly important in the description of the physical properties of low–mass AGBs, as described in details by Ventura & Marigo (2009) and Ventura & Marigo (2010). The interested reader may find in paper I a detailed discussion on how the modelling of the absorption coefficients in C–rich mixtures affects dust production by AGBs that reach the C–star stage.

We follow the nucleosynthesis evolution of 30 elements, from hydrogen to alluminum, with the most relevant isotopes entering the p-p and 3α chains, and the CNO cycle. The nuclear cross sections are taken from the NACRE compilation (Angulo et al. 1999), with a few exceptions, the most relevant for this study being the rate of the proton capture reaction by nitrogen nuclei, taken from Formicola et al. (2004).

The models presented in this work were calculated with an overall metallicity $Z = 0.008$, a helium content $Y = 0.26$, and a mixture scaled according to Grevesse & Sauval (1998), with an α−enhancement $[\alpha/{\rm Fe}] = +0.2$.

2.2 Dust production and the stellar wind

The scheme adopted to model the structure of the wind at a given phase during the AGB evolution is the same as in paper I, based on the description given in the series of papers by Ferrarotti & Gail (2001, 2002, 2006).

The wind is modelled via two differential equations describing the radial behaviour of the velocity of the gas and the optical depth. Indicating the mass, luminosity, effective temperature, radius, mass loss rate of the star with M, L, T_{eff}, R_*, and $\dot{M}$, we have:

$$v\frac{dv}{dr} = -\frac{GM}{r^2}(1 - \Gamma), \qquad (1)$$

$$\frac{d\tau}{dr} = -\rho k \frac{R_*^2}{r^2}, \qquad (2)$$

where

$$\Gamma = \frac{kL}{4\pi cGM}. \qquad (3)$$

Equations 1 and 2 are completed by the law of mass conservation:

$$\dot{M} = 4\pi r^2 \rho v, \qquad (4)$$

and by the radial variation of temperature in the approximation of a spherically simmetric, grey wind (Lucy 1976):

$$T^4 = \frac{1}{2}T_{\rm eff}^4 \left[1 - \sqrt{1 - \frac{R_*^2}{r^2}} + \frac{3}{2}\tau\right], \qquad (5)$$

where k is the flux–averaged extinction coefficient of the gas–dust mixture, and can be expressed as,

$$k = k_{\rm gas} + \sum_i f_i k_i, \qquad (6)$$

and $k_{\rm gas} = 10^{-8}\rho^{2/3}T^3$ (Bell & Lin 1994). The sum in eq. (6) is extended to all the dust species considered: the f_i terms give the degrees of condensation of the key–elements for each dust species, whereas k_i represent their corresponding extinction coefficients. This simple opacity law is used in the wind model since the AESOPUS tool does not give opacities for temperatures below 2000K. This is not an entirely correct use of the Bell & Lin (1994) formula, which of course adds physical inconsistency to the model. But since the gas opacity is typically much smaller than the overall dust opacity, the effects are small. In fact, it would have made little difference if we had assumed $k_{\rm gas} = 0$ instead, as we integrate from the condensation radius (where dust formation region starts and dust opacity dominates) out to a distance

$10^4 R_*$ away from the star (where the gas opacity is very low).

We consider the thermal gas pressure force to be negligible beyond the condensation radius, compared to the radiative acceleration. Hence, we omit the pressure term in the equation of motion, but assume that there is a nonzero flow over the inner boundary (we assume $v_0 = 2\text{km/s}$, which is similar to the expected sound speed) despite the fact that there is formally no gas pressure at the inner boundary. Obviously, this is physically inconsistent, but the effect on the results is usually small and assuming a nonzero flow speed at the inner boundary simplifies the numerical solution of equations (1-6) considerably. We note, however, that this assumption may be somewhat problematic for critical winds ($\Gamma \sim 1$), which are slow and may have outflow speeds which are comparable to the assumed sound speed at the inner boundary.

Dust growth takes place by vapour deposition on the surface of some pre-formed seed nuclei, assumed to be nano–meter sized spheres. The precise chemical nature of these seed grains is not important in what follows. We consider various types of dust, depending on the surface chemical composition of the star. In oxygen–rich winds, we consider olivine, pyroxene, quartz and iron grains, whereas for C–rich environments we account for the presence of solid carbon, silicon carbide and iron grains. For each condensate, we define a key element whose abundance is the minimum among all the elements necessary to form the corresponding dust aggregate. Silicon is the key element for olivine, pyroxene, quartz and silicon carbide, whereas iron and carbon are the key elements for iron dust and solid carbon. All the species considered, with the corresponding condensation reactions and key–elements, are listed in Table 1.

The growth rate of each dust species depends on the competition between the formation and destruction rates. The former is evaluated on the basis of the number density of the key–element and the thermal velocity of the corresponding molecule, whereas the latter is calculated via the difference between the formation enthalpy of the dust species and of the individual molecules concurring to the formation process. All the references concerning the thermodynamic quantities considered can be found in paper I.

The regions close to the central star are generally too hot to allow for dust condensation, the destruction rate exceeding by far the production rate. At a distance of 3-4 stellar radii from the surface of the star, the temperature drops below 1000 K, and dust formation occurs. The consequent increase in the opacity accelerates the wind via the strong radiation pressure, and halts dust formation. We therefore expect the sizes of the different grain species and the terminal velocity of the wind to reach an asymptotic behaviour.

Because the assumed initial dimension of the grains, a_0, is much smaller than the size reached by the various grains in the asymptotic regime, the results are practically independent of the choice for a_0: simulations based on different values for a_0 (still in the nano-sized regime) lead to the same result.

A further initial condition, imposed by the lack of a nucleation theory to be applied for any of the dust species considered, is the initial density of seed grains, n_d. In agreement with paper I, we assume $n_d = 3 \times 10^{-13} n_H$ (note that in Section 2.2.2 of paper I, due to a typo, it is given
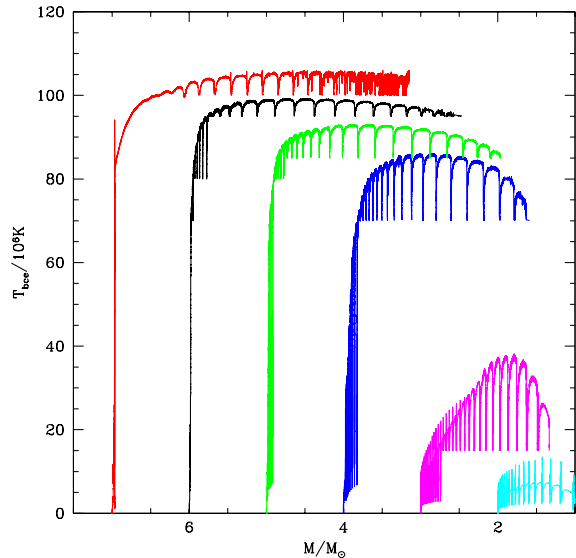
Figure 1. Variation during the Thermal pulses phase of the temperature at the bottom of the external convective zone as a function of the total stellar mass of models with initial mass 7 M$_\odot$ (red), 6 M$_\odot$ (black), 5 M$_\odot$ (green), 4 M$_\odot$ (blue), 3 M$_\odot$ (magenta), 2 M$_\odot$ (cyan). Note that models experiencing HBB keep the same temperature for the vast majority of the time during which they undergo the strongest mass loss.

$n_d = 3 \times 10^{-4} n_H$ instead), which, as order of magnitude, reflects the typical number densities of grains in the outflows of AGBs (Knapp 1985). A higher n_d, for a given size of the grains, corresponds to a higher degree of condensation of the key–species into dust, and consequently to a smaller density of the various molecules in the wind (see Ferrarotti & Gail (2006), Eq.20–30). This is not relevant as far as the degree of condensation is small, and has the largest impact in those cases where dust condensation is most efficient: i.e. the SAGB models presented here, which we will see is the most efficient producers of dust. A change in n_d by a factor 2 determines a variation in the grain size of the order of $\sim 10\%$.

To summarize, the amount of dust produced and its composition are mainly determined by the following quantities:

(i) The physical parameters of the central star and, in particular, the luminosity, effective temperature and the mass loss rate; these determine the radial variation of the thermodynamics of the wind.

(ii) The surface chemistry of the star, that is relevant in the determination of the dominant dust species (either silicates or carbon dust, according to the C/O ratio), and in the quantity of dust formed (via the mass fractions of the key–elements).

(iii) The description of the absorption and scattering processes for the various elements, that determine the extinction coefficient.

Table 1. Dust species considered in the present analysis, their formation reaction and the corresponding key–elements (see text).

Grain Species	Formation Reaction	Key–element
Olivine	$2x\mathrm{Mg} + 2(1\text{-}x)\mathrm{Fe} + \mathrm{SiO} + 3\mathrm{H}_2\mathrm{O} \rightarrow \mathrm{Mg}_{2x}\mathrm{Fe}_{2(1-x)}\mathrm{SiO}_4 + 3\mathrm{H}_2$	Si
Pyroxene	$x\mathrm{Mg} + (1\text{-}x)\mathrm{Fe} + \mathrm{SiO} + 2\mathrm{H}_2\mathrm{O} \rightarrow \mathrm{Mg}_x\mathrm{Fe}_{(1-x)}\mathrm{SiO}_3 + 2\mathrm{H}_2$	Si
Quartz	$\mathrm{SiO} + \mathrm{H}_2\mathrm{O} \rightarrow \mathrm{SiO}_2(s) + \mathrm{H}_2$	Si
Silicon Carbide	$2\mathrm{Si} + \mathrm{C}_2\mathrm{H}_2 \rightarrow 2\,\mathrm{SiC} + \mathrm{H}_2$	Si
Carbon	$\mathrm{C} \rightarrow \mathrm{C}(s)$	C
Iron	$\mathrm{Fe} \rightarrow \mathrm{Fe}(s)$	Fe

3   THE EVOLUTIONARY PROPERTIES OF AGB AND SAGB MODELS WITH $Z = 0.008$

The main physical features of the evolution of AGB stars are discussed in the reviews by Karakas (2011), Herwig (2005); further details on the efficiency of the TDU and the achievement of the C–star stage can be found in Stancliffe et al. (2004), Stancliffe et al. (2005), Karakas et al. (2010) (and references therein). An exhaustive description of the SAGB phase can be found in the classic paper by Garcia-Berro et al. (1997), and the more recent investigations by Gil–Pons et al. (2007), Siess (2007, 2010).

Here we provide a brief description of the main features of the evolution of the AGB and SAGB stars with initial metallicity $Z = 0.008$, that prove essential in the understanding of the dust formation process.

The threshold mass separating the AGB and SAGB regimes is $6.5\mathrm{M}_\odot$. Less massive models evolve on a CO core, whereas higher masses undergo off–center carbon ignition, and eventually develop a degenerate core, made up of oxygen and neon. This finding is partly dependent on the amount of overshoot from the convective core: when the extra–mixing is neglected, the above limit shifts upwards by $\sim 1\mathrm{M}_\odot$.

Ventura & D'Antona (2005) outlined the key role played by the treatment of the convection in the extent of HBB, i.e. the nuclear activity that develops at the bottom of the convective envelope once the temperature exceeds $30 - 40$ MK. The FST modelling of convection, used in the present work, leads easily to HBB conditions for models whose initial mass exceeds a threshold value (D'Antona & Mazzitelli 1996; Ventura & D'Antona 2005) that depends on the metallicity of the star and on the assumptions concerning the overshoot from the border of the convective core during the two major phases of hydrogen and helium burning. The relevance of HBB in this context is twofold: a) even in moderate HBB conditions carbon is destroyed in the envelope of the star, thus leaving the only possibility for the formation of silicate–type dust; b) HBB is accompanied by an increase in the luminosity of the star, which, given the steep dependence on luminosity of the Blöcker's mass loss description ($\dot{M} \propto M^{3.7}$), favours a higher rate of mass loss; the relationship between $\dot{M}$ and density of the gas in the wind (see Eq.4), will make dust formation seem more efficient[1].

The variation during the AGB (or SAGB) phase of the

temperature at the bottom of the convective envelope of models differing in their initial mass is shown in Fig. 1. The choice of the mass of the star as abscissa allows to identify the physical conditions at the time when most of the mass loss occurs. We can clearly identify a threshold mass of 3.5 $\mathrm{M}_\odot$ separating the more massive objects, experiencing HBB, from their lower mass counterparts, whose temperature at the bottom of the convective envelope remains below 40 MK. Interestingly, we note that models experiencing HBB maintain an approximately constant temperature during most of the time when they loose their mass: this allows us to understand the nucleosynthesis experienced, and the corresponding variation of the surface chemistry.

To understand the effects of the initial metallicity of the stars on the HBB phenomenology, in the left panel of Fig. 2 we show, for each star, the temperature at the bottom of the surface convective zone and the peak luminosity during the AGB evolution, which, in turn, is related to the core mass of the star. Models discussed in the present work are indicated as open squares, whereas the $Z = 0.001$ models analyzed in paper I are represented by full triangles.

Lower Z models evolve, for a given core mass (luminosity) at higher temperatures, thus allowing a stronger nucleosynthesis at the bottom of the convective envelope. This difference is confirmed in the right panel of Fig. 2, showing the evolution of the surface oxygen with mass for models of different initial mass and metallicity $Z = 0.008$ and $Z = 0.001$. To illustrate the extent of oxygen depletion, we report in the ordinate the ratio of the surface oxygen mass fraction to its initial value. All the $Z = 0.008$ models experiencing HBB (M $> 3.5\mathrm{M}_\odot$) achieve only a modest depletion of the surface oxygen, in comparison to their lower Z counterparts which, in some cases, reduce the oxygen in their envelope by a factor ~ 10. For both metallicities, the strongest depletion is reached for masses still in the AGB regime; in SAGBs mass loss rates and oxygen depletion proceed with comparable timescales: these stars loose a high percentage of their mass before a strong depletion of the surface oxygen is achieved (Ventura & D'Antona 2011).

In models with M $\lesssim 3\mathrm{M}_\odot$, not experiencing any HBB, we expect only a poor, if any, production of silicates, because the mass loss rates are extremely small, thus preventing the possibility that a radiation pressure driven wind develops.

The possibility for these stars to form dust is related to the TDU. A highly efficient TDU drives the bottom of the envelope to regions previously enriched by 3α nucleosynthesis; the consequent increase in the carbon content in the envelope eventually leads to the C–star stage: this would

---

[1] Note that this result is a consequence of the scheme we follow, i.e. adopting an empirically determined mass loss treatment, and finding out the dust formed accordingly. As stated in Sect.2, the correct treatment would be to determine the mass loss rate on the basis of the dust formed
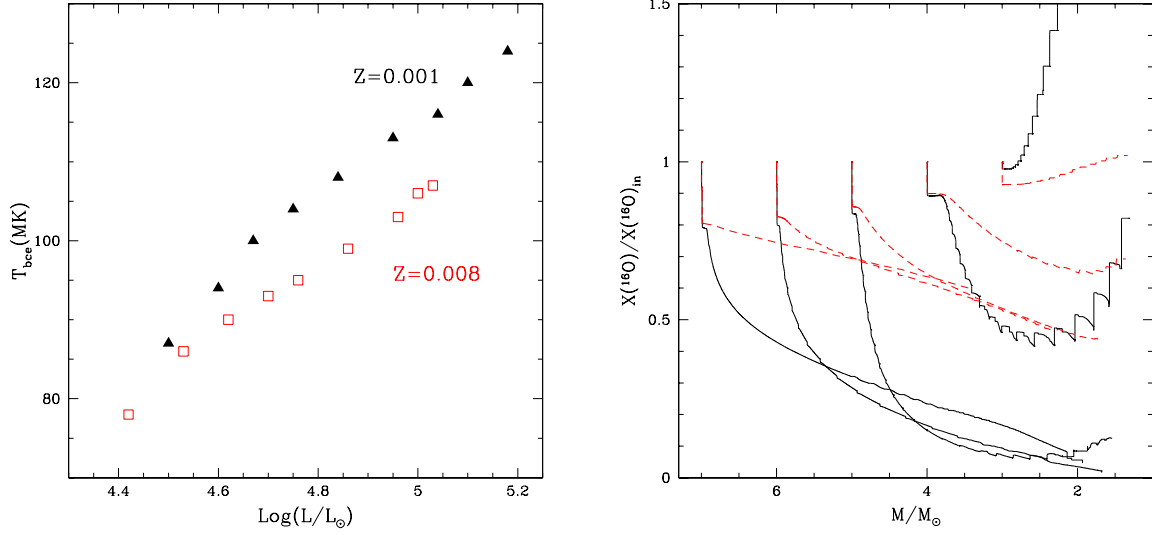
Figure 2. *Left panel*: the average temperature at the bottom of the convective envelope as a function of the peak luminosity reached during the Thermal Pulses phase in AGB and SAGB models of metallicity $Z = 0.008$ studied in the present investigation (open squares) and those presented in Ventura & D'Antona (2009, 2011) (red,full triangles). *Right panel*: surface oxygen mass fraction (divided by the initial abundance) as a function of the stellar mass for the models with $Z = 0.001$ discussed in paper I (solid, black), and the models presented here (dashed, red).
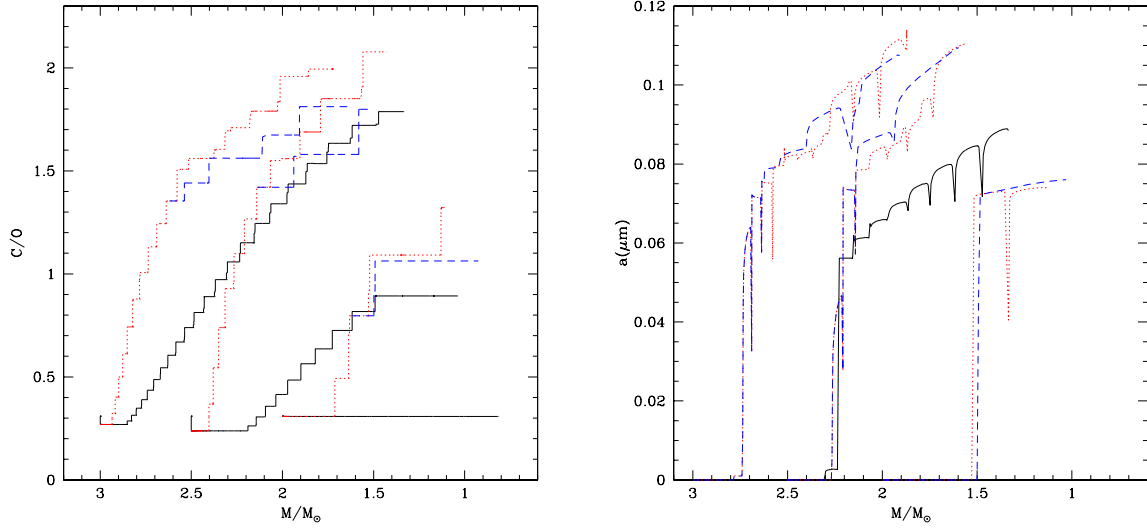
Figure 3. Left: The variation of the C/O ratio in $Z = 0.008$ models not experiencing HBB, with initial masses 2,2.5, and 3$M_\odot$. Lower mass models are not shown, since they do not experience any TDU in any case. The solid lines (black) indicate the results obtained when the borders of the convective region developed during each Thermal Pulse is fixed via the Schwarzschild criterium; dotted (red) lines indicate the evolution when a small extra-mixing is assumed (see text for details). Dashed, blue lines indicate the variation of the C/O ratio when extra–mixing is adopted, and mass loss during the C–star stage is modeled with the treatment by Wachter et al. (2008). Right: The variation of thi size of carbon grains in the same models presented in the left panel.
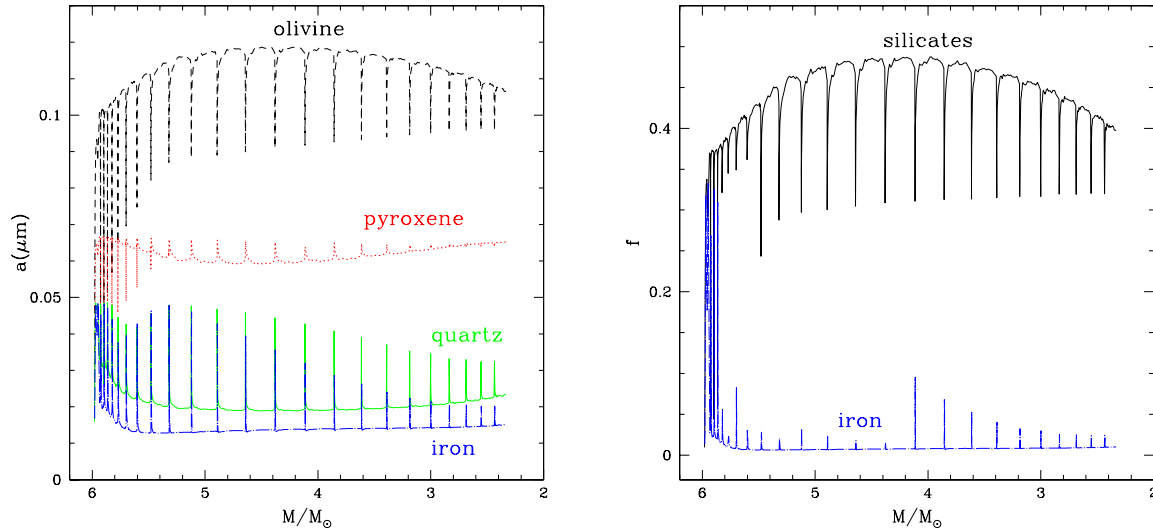
Figure 4. *Left panel*: variation of the size of different grain species formed during the AGB evolution of a model with initial mass 6M$_\odot$: olivine (dashed, black), pyroxene (dotted, red), quartz (solid, green), and iron (dot–dashed, blue). *Right panel*: the fraction of silicon condensed into silicates (solid, black), and the fraction of iron condensed into iron grains (dot–dashed, blue) for the same 6M$_\odot$ stellar model.

eliminate the oxygen needed to form silicates, and favour the formation of carbon dust[2].

The issue of forming carbon stars is a long-standing problem for stellar evolution theories. On the observational side, the investigations by Groenewegen & de Jong (1993), Marigo et al. (1999), Izzard et al. (2004), indicated the core mass at which TDU must begin, and the efficiency of the inwards penetration of the convective mantle required to reproduce the luminosity function of carbon stars in the Magellanic Clouds. Most of the evolution codes fail to achieve this result, because the TDU begins late during the AGB evolution, with an efficiency smaller than required by the observations (Mowlavi 1999; Herwig 2000). Due to the extreme sensitivity of the results to the details of the numerical treatment of the convective borders (e.g. the modality with which the convective/radiative interface is determined, the spatial zoning near the convective boundaries), the results obtained by various research groups are substantially different (Straniero et al. 1997). An important step forward was made by Stancliffe et al. (2005), that using a fully implicit and simultaneous solution of the equations of stellar structure, nuclear burning, and diffusive mixing, could reproduce the luminosity function of carbon stars in the LMC, with no need of any free parameter.

The models produced by our code, where the boundaries of convective regions is determined via a straight application of the Schwartzschild criterium (i.e. $\zeta = 0$), share the difficulty of obtaining a TDU with the required efficiency. As

can be seen in the left panel of Fig.3 (solid lines), that shows the evolution of the surface C/O ratio, the C-star stage is reached only by models with initial mass M=2.5,3M$_\odot$, in a late phase of the AGB evolution. On the other hand, to confirm the importance of the treatment of convective boundaries, we have shown that even a modest extra-mixing from the convective shell formed during the TP leads to very different results: the results indicated with dotted tracks in Fig.3 were obtained with $\zeta = 0.001$, much smaller than the values invoked to describe overshoot from the borders of the convective cores during the main sequence phase (i.e. $\zeta = 0.02$). The impact of the assumed extra–mixing can be understood by the comparison with the solid lines. The choice $\zeta = 0.001$ favours the achievement of the C–star stage for the stars with initial mass between 2M$_\odot$ and 3M$_\odot$, reported in Fig. 3. We note that even a tiny overshoot from the shell developed during each TP is sufficient to induce a deep TDU, which leads to a C/O ratio exceeding unity (the essential condition to produce solid carbon and silicon carbide) after a few TPs, when only a $\sim 5 - 10\%$ of the stellar mass is lost. With the present choice concerning ζ, we find that stars with mass below 1.5M$_\odot$ never become carbon stars.

A detailed tuning of the amount of extra-mixing needed to account for the observations is beyond the scope of the present investigations; we limit here to stress the sensitivity of the results to this choice, and we will describe how the dust formation process also depends on ζ.

---

[2] When C/O$>$ 1, all the oxygen available is locked into CO molecules, which are highly stable, due to their large dissociation energy.

4 DUST PRODUCTION

The results discussed in the previous section indicate that one of the main findings of paper I holds also at higher metallicites: stars whose initial mass is above the threshold value to allow HBB conditions produce silicates, whereas lower mass objects produce carbon–rich dust.

We show in the left panels of Fig. 4 the size of the dust grains formed around a typical model experiencing HBB, with an initial mass M = 6M$_\odot$. Olivine is the dust species most easily formed, followed by pyroxene, and by small quantities of quartz and iron. The spread between the size of the olivine grains and of the other elements gets larger as the star evolves on the AGB. This is because the increase in the mass loss rate is associated with a more efficient production of olivine; this, in turn, determines a faster acceleration of the wind, that prevents the formation of the other species. Note the periodic drop in the size of the olivine grains, when TPs occur, and the star looses mass more slowly.

In the right panel of Fig. 4 we show, for the same 6M$_\odot$ stellar model, the fractions of silicon and iron condensed into dust. In the present set of $Z = 0.008$ models the production of silicates continues for the whole AGB evolution; this is different compared to paper I, where it is shown that in massive AGBs silicates production stops (see paper I, left panel of Fig. 3). This difference can be understood from the right panel of Fig. 2, showing that surface oxygen destruction is much softer in the present models than at lower Z. Unlike the $Z = 0.001$ stars, here we never enter the situation in which water, one of the key ingredients to form the silicates (see Table 2.2), is consumed, and therefore the production of the silicates never stops.

Since olivine is the most abundant species, we may understand the trend with stellar mass of the amount of silicates formed by comparing the size of the olivine grains in the surroundings of AGB stars of different initial mass. This is shown in Fig. 5.

Higher mass models evolve at large luminosities. Given the steep slope of the $\dot{M}(L)$ relationship provided by the Blöcker's description, mass loss will proceed faster. Because we keep the velocity constant until the point where dust formation becomes possible (i.e. where for at least one of the species considered the production term exceeds destruction), we find via Eq.4 a larger gas density there. This favours dust formation by increasing the number density of all the molecules entering the various sublimation reactions. More massive models are therefore expected to produce grains with larger size, as confirmed by the trend shown in Fig. 5. The fraction f$_{sil}$ of silicon condensed into dust ranges from 35% at M=3.5$M_\odot$ up to 50% in the SAGB regime. Because a great production of silicates affects iron condensation, the trend with mass of the fraction of iron condensed is opposite: f$_{ir}$ varies from 10% at low M, down to $\sim$ 2% for SAGBs.

The grain sizes obtained here for olivine (see figures 4 and 5) are marginally consistent with the grain sizes required to drive a wind according to Höfner (2008), but we note also that the grain sizes obtained at lower metallicity (paper I) are significantly smaller, which indicate some tension between our results and the grain-size requirement derived by Höfner (2008). The predictions by Höfner (2008) have very recently been confirmed observationally by Norris et al. (2012), which also seems to rule out any significant
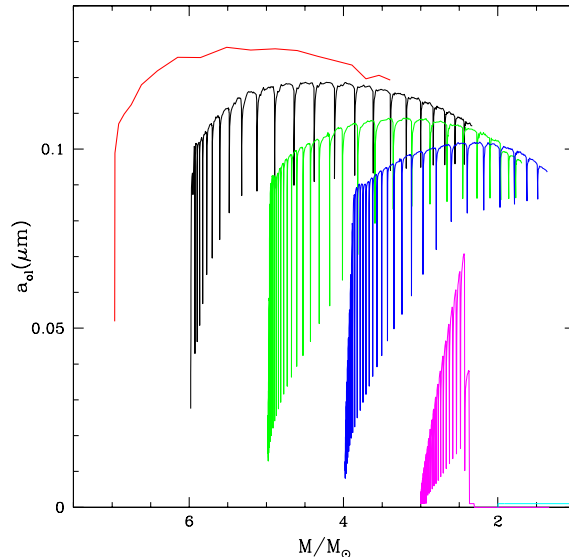
Figure 5. Variation during the AGB (or SAGB) evolution of the size of olivine grains formed around stars with different initial mass that experience HBB. The color code is the same of Fig. 1.

production of iron–rich silicates. However, the latter may in part explain the discrepancy with our results, since iron–free silicates have clearly different optical properties (lower opacity) that may favour growth to large sizes as they are not heated by radiation as much as iron–rich silicates.

The larger depletion of surface oxygen in more massive stars has a negligible role here, because the abundance of the key element for silicates, i.e. silicon, remains almost constant in all cases[3].

Stellar models not experiencing HBB achieve only a modest production of silicates, because the density of the key–species declines very rapidly away from the surface of the star. This can be seen in Fig. 5, where we note the small olivine grain sizes formed by the 3 M$_\odot$ model. The possibility that carbon–type dust is produced depends on the extent of the extra–mixing from the convective shell driven by the thermal pulse. We see from Fig. 3 that when overshooting is not considered, it is only in the 3 M$_\odot$ model that the condition to produce carbon dust, i.e. C/O> 1, is met. The situation changes in the presence of even a modest amount of extra–mixing (i.e. $\zeta = 0.001$). In such case, TDU becomes much more efficient and penetrating, and the stars not experiencing HBB reach the C–star stage, producing carbon–type dust. The fraction of carbon condensed into dust, of the order of $f_C \sim 0.1$, is smaller than predicted by more detailed models of dust–driven mass loss (see e.g. Mattsson

---

[3] The possibility that surface silicon increases in the AGB models experiencing the strongest HBB is discussed in Ventura, Carini & D'Antona (2011), who however find a modest (if any) increase in the silicon mass fraction, that would have only a negligible impact on the results presented here.
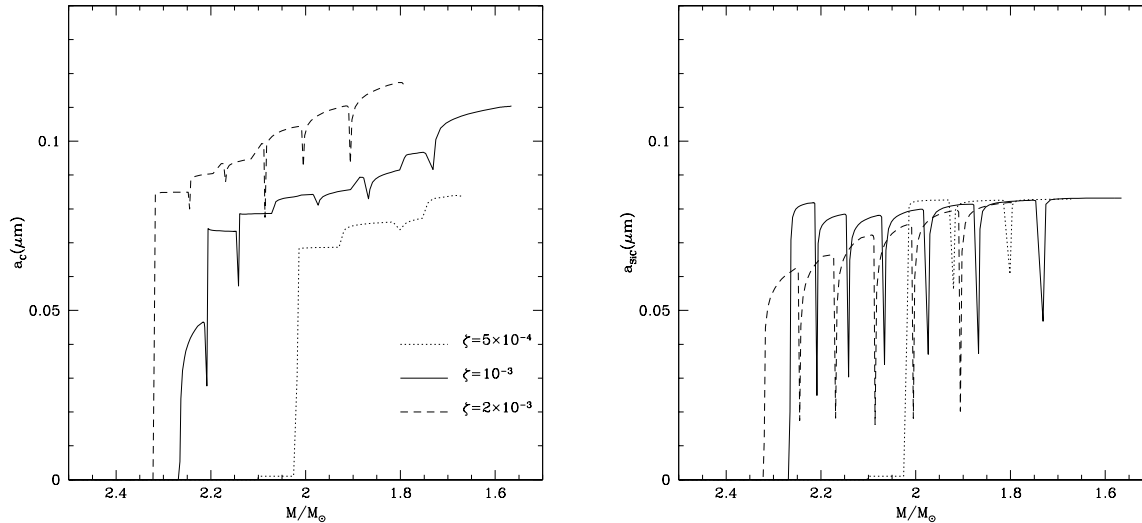
Figure 6. The variation of the size of solid carbon (left) and SiC (right) grains formed during the evolution of a model of initial mass 2.5M$_\odot$. The three lines indicate the results corresponding to various assumptions for the extra–mixing from the borders of the convective shell that develops following each TP.

& Höfner (2011)). This is partly due to the small extent of the extra–mixing assumed during the TDU, that prevents great enhancements of the surface carbon.

5 HOW ROBUST ARE THE PRESENT RESULTS?

The results found in terms of the type, total mass, and grain size distribution of the dust particles formed around AGBs depend on many assumptions made to calculate the evolutionary sequences, associated with the details of the AGB modelling and the description of the dust formation process.

5.1 The physical inputs for the AGB description

In paper I (section 5) we explored how the results obtained depend on the assumptions in the macro–physics adopted to describe the AGB evolution, i.e the treatment of convection (both the efficiency of the convective transport and the treatment of convective borders) and the mass loss prescription.
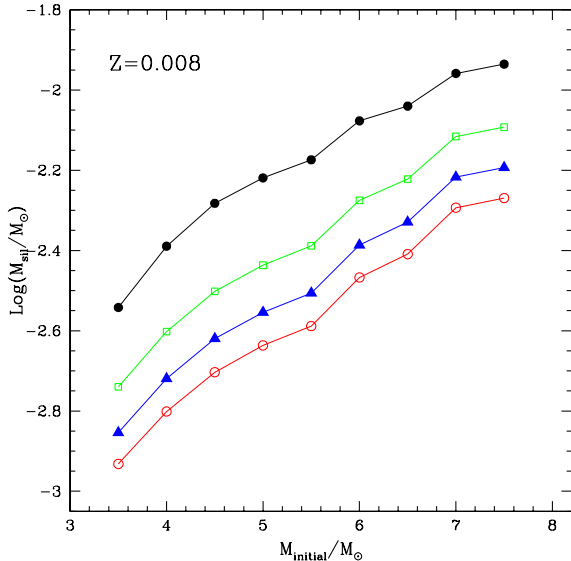
The convection model is still the main source of uncertainty in the more massive models, because it determines the extent of the HBB experienced, and thus the surface evolution of two key–elements for the dust formation process, i.e. carbon and oxygen. Use of a lower convection efficiency would increase the threshold mass separating the stars predicted to form silicates from those producing carbon grains.

For the models not undergoing HBB, the treatment of the convective borders is the key–issue in determining how much dust is formed in their surroundings. In the present work, the possible overshoot of the convective eddies into the regions radiatively stable is described by the parameter

ζ (see Sect. 2.1). The two panels of Fig. 6 show the effects of changing ζ on the size of the solid carbon (left panel) and SiC (right panel) grains. The results refer to a 2.5M$_\odot$ model, in the range of masses experiencing TDU. We see that an increase in ζ by a factor 2 leads to formation of carbon grains that are 10–20% bigger. In terms of the amount of dust formed, for the three models discussed we find masses of solid carbon (the main dust component in the present case) of $2.8 \times 10^{-4} M_\odot$, $6.4 \times 10^{-4} M_\odot$, $9 \times 10^{-4} M_\odot$, for $\zeta = 5 \times 10^{-4}$, 10^{-3}, 2×10^{-3}, respectively. These results suggest that the extension of the convective shell formed at each TP has a critical impact on the amount of carbon–dust formed in AGBs experiencing TDU, and is the main source of uncertainty for the predictive power of this work.

Mass loss was also shown to be a source of uncertainty in paper I, because use of a prescription with a milder dependence on the luminosity than the Blöcker's recipe (e.g. the formulation by Vassiliadis & Wood (1993)) would lead to a lower production of silicates: this would greatly affect the resultant dust yields found, because the stars would loose only a tiny fraction of their envelope by the time that the surface oxygen is consumed, so that most of the mass lost would be oxygen–poor, which prevents the formation of silicates. We note that this effect would be of smaller importance here, because the extent of HBB is softer, such that the oxygen is not severely depleted (see the right panel of Fig.2).

To investigate also how the treatment of mass loss influences the production of carbon–rich dust in models of smaller mass, we calculated models that reach the C–star stage (initial masses 2, 2.5, 3M$_\odot$) with the mass loss formulation by Wachter et al. (2008). This treatment is particularly suitable for our purposes, because it is based on the same metallicity as the models presented here (Z=0.008),

For silicate grains, the uncertainty associated to the refractive index is still large and it is important to estimate how this affects the predicted mass of dust formed by AGB and SAGB stars. We therefore repeat our analysis adopting different sets of silicates refractive index currently available in the literature, such as the optical properties of the astronomical silicates by Draine & Lee (1984), the empirically determined efficiencies by Jones & Merrill (1976), the optical constants by Ossenkopf et al. (1992), and the invidual properties for each of the three silicates considered here, i.e. olivine (Dorschner et al. 1995), pyroxene (Jager et al. 1994), and quartz (Brewster 1992). A detailed analysis of the differences among these data can be found in Jeong et al. (2003) (see their Figs. 2 and 3). Here we simply compare the results that we obtain for the total mass of silicates produced, restricting the comparison to stars with mass $M \geqslant 3.5 \ M_\odot$ that experience HBB.

The results are shown in Fig. 7. The largest mass of silicates is predicted to form when the data from Dorschner et al. (1995) are used, whereas the description by Jones & Merrill (1976) provides the lowest silicates production. We note that, independently of the initial mass of the star, the difference is within ~ 0.4 dex; we assume this to be the degree of uncertainty due the choice of the refractive index.

Figure 7. The total mass of silicates produced by AGB and SAGB models experiencing HBB. The various symbols indicate the results obtained with different sets of optical properties: open (red) circles Jones & Merrill (1976); full (blue) triangles Ossenkopf et al. (1992); open (green) squares Draine & Lee (1984); full (black) dots Dorschner et al. (1995) (olivine), Brewster (1992) (quartz), and Jager et al. (1994) (pyroxene).

and is aimed at determining the rate of mass loss for AGB stars already in the C–star phase.

The treatment by Wachter et al. (2008) predicts that during the C–star phase mass is lost faster in comparison to the Blöcker prescription, because of the large negative exponent of the effective temperature in the Wachter et al. (2008) formulation (see their Eq.1). The star experiences a smaller number of thermal pulses, which prevents the achievement of large C/O ratios. This can be clearly seen in the left panel of Fig. 3, where evolutions calculated by means of the Wachter et al. (2008) formula are shown with dashed lines, to be compared with the dotted tracks. We note in the right panel that the amount of solid carbon formed is similar in the two cases, because the effects of the larger abundance of surface carbon achieved by the Blöcker's models are partly compensated by the smaller mass loss rate experienced, which, in agreement with our scheme, leads to a smaller production of dust.

5.2 The optical properties of silicates

The quantity Γ, defined in Eq. 3, represents the coupling between matter and radiation field. The increase in Γ when dust begins to form leads to an increase in the radiation pressure, with the consequent acceleration of the wind, that halts the dust formation process.

The interaction between the radiation and the dust grains is expressed by the coefficient k, which, in turn, depends on the optical properties of the type of dust formed.

6 DISCUSSION

The predicted mass of dust produced by AGB and SAGB stars with $Z = 0.008$ is reported in Table 2, where we also specify the mass of the individual dust species. For the silicates we used the set of optical constants by Ossenkopf et al. (1992). In Fig. 8, we show separately the predicted mass of silicates (left panel) and carbon–rich dust (right panel) for each stellar mass. Filled circles indicate the mass of dust produced by the models presented in this work, while open squares represent the $Z = 0.001$ models discussed in paper I. For comparison, we also show the dust mass predicted by Ferrarotti & Gail (2006) for the same two metallicities (open triangles $Z = 0.001$; filled triangles $Z = 0.008$).

The large production of silicates in higher–mass models, found in paper I for $Z = 0.001$, is confirmed at $Z = 0.008$. The two lines in the left panel of Fig. 8, corresponding to the two metallicities, follow similar trends, and show a drop for masses $M < 3.5 \ M_\odot$ that do not experience any HBB. The discontinuity at $3.5 \ M_\odot$ would be smaller without overshoot from the shell (see the open points). Z=0.008 models produce a mass of silicate–type dust a factor ~ 10 larger compared to the $Z = 0.001$ case. This reflects the difference in metallicity, that results in a higher density of silicon in the wind. The trend of dust formed with stellar mass is monotonic here, as opposed to the $Z = 0.001$ models (note the local minimum for Z=0.001 at M=5M$_\odot$), because the HBB is softer. Thus we never reach a situation where shortage of water molecules inhibits silicates formation.

Comparing the mass of silicates predicted by our models with the results by Ferrarotti & Gail (2006) at the same stellar metallicity, we note that the difference is smaller at $Z = 0.008$ than at $Z = 0.001$. In fact, the higher metallicity prevents (or delays) the achievement of the C–star stage, so that in the more massive stars silicates are produced independently of the physical input used to model the AGB
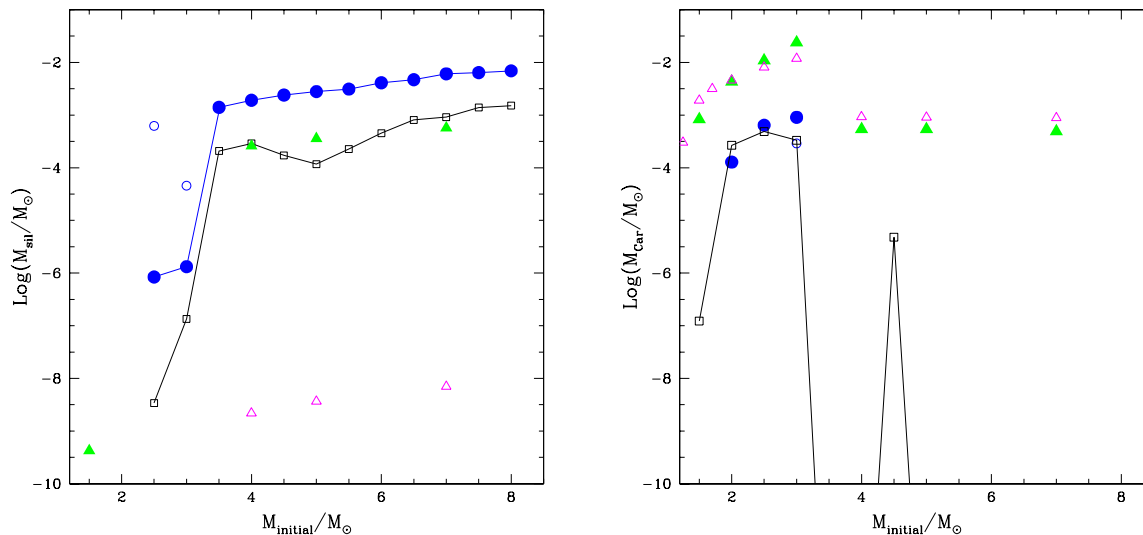
Figure 8. Total mass of silicates (*left panel*) and carbon dust (*right panel*) produced by the stellar models presented in this paper (blue filled dots) and by the $Z = 0.001$ models published in paper I (black open squares). For comparison, we also show the results by Ferrarotti & Gail (2006) at metallicites $Z = 0.001$ (magenta open triangles) and $Z = 0.008$ (green filled triangles). The two open points in the left panel show what would be the mass of silicates produced by the two lowest mass models with $Z = 0.008$ if the overshoot from the convective shell were to be neglected (see the text).

evolution. Still, comparing the filled circles and the filled triangles, we note that the mass of silicates predicted by our models is larger because (*i*) the HBB experienced is stronger and (*ii*) the production of silicates in the models by Ferrarotti & Gail (2006) is limited to the first part of the evolution, before the star enters the C–star stage. The results by Ferrarotti & Gail (2006) do not show the same proportionality of the mass of silicates formed with metallicity.

The right panel of Fig. 8 shows that for the models presented in this paper we do not find any carbon–type dust for $M \geqslant 3.5\ M_\odot$, because the HBB destroys the surface carbon. This is at odds with the results by Ferrarotti & Gail (2006), where some carbon–type dust is produced at all stellar masses. For carbon–type dust, the mass predicted by our models show a negligible dependence on the initial stellar metallicity. In fact, dust production is mainly sensitive to the amount of carbon formed in the 3α burning shell and dredged–up to the surface; such nucleosynthesis is scarcely dependent on the initial metal content of the star, unlike the CNO burning at the bottom of the envelope, which is sensitive to the initial abundances of silicon, magnesium and oxygen.

The models by Ferrarotti & Gail (2006) predict a larger mass of carbon–type dust for low–mass stars, because of the different assumptions concerning the extent of the TDU. Part of the difference is also due to the low–T surface opacities used by the synthetic models upon which the AGB evolution by Ferrarotti & Gail (2006) is computed: they are based on a solar-scaled mixture, where any variation in the C/O ratio is neglected. As shown by Marigo (2002), when C/O exceeds unity, CN and C_2 molecules replace water as

the main absorbers of radiation, which, in turn, leads to an increase in the opacity for regions with temperatures below 3000K. Because a higher opacity favours cooling and expansion of the external layers, this will reflect into an increase in the rate at which mass loss occurs. In our models we therefore expect that less carbon is formed, because the star looses its envelope more rapidly.

Fig. 9 shows the total mass of dust produced by stars with different initial mass and metallicity. Compared to Ferrarotti & Gail (2006), our models show an opposite trend with stellar mass, which is both qualitative and quantitative: more massive models produce more dust, under the form of silicate–type grains, whereas in the Ferrarotti & Gail (2006) case most of the dust is produced by low–mass stars, and as carbon dust. In addition, our models appear to be extremely sensitive to the initial stellar metallicity, with higher Z models producing more dust. On the contrary, the mass of dust predicted by Ferrarotti & Gail (2006) is relatively constant with Z, because the surface–carbon abundance in those models is mostly dependent on the nucleosynthesis in the shell that forms during the thermal pulse.

6.1 Implications for the cosmic dust yields

Following the analysis done in paper I, we can investigate the implications of the above findings for the cosmic dust enrichment contributed by intermediate mass stars. To do this, we assume that all the stars form in a single burst at a reference initial time with metallicity $Z = 0.008$ and according to a Larson initial mass function (IMF) with stellar mass in the range $[0.1 - 100]$ $M_\odot$ and a characteristic stellar mass of $m_{ch} = 0.35 M_\odot$ (see equations 20 and 21 in paper I

Table 2. Dust mass produced by AGB and SAGB models of metallicity $Z = 0.008$. The initial stellar mass M is reported in the first column. The total mass of dust, M_{d} and the mass of olivine (M_{ol}), pyroxene (M_{py}), quartz (M_{qu}), solid iron (M_{ir}), solid carbon (M_{C}) and silicon carbide (M_{SiC}) are also shown. All the masses are expressed in solar units. The optical constants from Ossenkopf et al. (1992) were used for the silicates. The three sets of models differ in the mass loss treatment (we used the recipes from Blöcker (1995) and Wachter et al. (2008)) and the treatment of the convective borders (expressed by the parameter ζ).

M	M_{d}	M_{ol}	M_{py}	M_{qu}	M_{ir}	M_{C}	M_{SiC}
				Blöcker $- \zeta = 0.001$			
1.5	1.15D-05	4.97D-07	1.89D-07	6.97D-08	1.06D-05	1.23D-07	3.85D-08
2.0	1.46D-04	1.01D-12	6.72D-13	3.22D-13	1.85D-05	1.28D-04	0.00D+00
2.5	8.30D-04	5.46D-07	2.06D-07	8.95D-08	1.89D-06	6.42D-04	1.86D-04
3.0	1.14D-03	7.54D-07	3.95D-07	1.67D-07	2.60D-06	9.06D-04	2.33D-04
3.5	1.41D-03	1.03D-03	3.22D-04	4.94D-05	7.77D-05	0.00D+00	0.00D+00
4.0	1.92D-03	1.44D-03	4.19D-04	4.52D-05	6.62D-05	0.00D+00	0.00D+00
4.5	2.41D-03	1.87D-03	5.00D-04	3.86D-05	5.43D-05	0.00D+00	0.00D+00
5.0	2.80D-03	2.20D-03	5.53D-04	3.69D-05	4.57D-05	0.00D+00	0.00D+00
5.5	3.12D-03	2.50D-03	5.88D-04	3.64D-05	4.21D-05	0.00D+00	0.00D+00
6.0	4.11D-03	3.47D-03	6.16D-04	1.95D-05	2.24D-05	0.00D+00	0.00D+00
6.5	4.69D-03	4.07D-03	5.93D-04	2.36D-05	2.52D-05	0.00D+00	0.00D+00
7.0	6.07D-03	5.49D-03	5.68D-04	1.26D-05	2.10D-05	0.00D+00	0.00D+00
7.5	6.41D-03	5.82D-03	5.76D-04	1.36D-05	2.35D-05	0.00D+00	0.00D+00
8.0	6.92D-03	6.11D-03	6.40D-04	1.70D-05	2.64D-05	0.00D+00	0.00D+00
				Blöcker $- \zeta = 0$			
2.0	2.40D-04	1.99D-14	1.23D-14	4.95D-15	2.40D-04	0.00D-00	0.00D+00
2.5	8.00D-04	4.30D-04	1.49D-04	4.52D-05	1.75D-04	0.00D-00	0.00D-00
3.0	6.43D-04	2.90D-05	1.15D-05	5.11D-06	4.72D-05	2.89D-04	2.61D-04
				Watcher (2008) $- \zeta = 0.001$			
2.0	1.88D-04	2.20D-12	1.01D-12	4.81D-13	4.77D-05	1.40D-04	0.00D+00
2.5	8.74D-04	7.90D-07	2.06D-07	8.95D-08	1.89D-06	6.73D-04	1.98D-04
3.0	1.03D-03	1.09D-06	3.95D-07	1.67D-07	2.60D-06	7.93D-04	2.31D-04

and Valiante et al. 2009). The cosmic dust yield of stars with masses $M \leqslant 8 M_{\odot}$, i.e. the total dust mass injected into the interstellar medium by AGB and SAGB stars normalized to the total mass of stars formed in the burst, evolves on stellar evolutionary timescales (see Fig. 10, right panel). The dotted and dashed lines indicate the separate contributions of carbon and silicate dust. For comparison, we show in the left panel the same quantities obtained for $Z = 0.001$ stars[4].

At the end of their evolution, intermediate mass stars with higher metallicity produce a cosmic dust yield that is a factor ~ 4.4 larger than that associated with their lower metallicity counterparts. In addition, when $Z = 0.008$ stars are considered, the dust mass is dominated by silicates at all times. The small carbon dust yields produced by stars with masses $\leqslant 3 M_{\odot}$ is not compensated by the higher frequency of low-mass stars obtained with the adopted stellar IMF. Conversely, the large silicate dust yields produced by more massive stars leads to a prompt enrichment on timescales $\geqslant 40$ Myr and, at ~ 100 Myr after the burst, the mass of silicate dust produced by $Z = 0.008$ stars is more than a factor 10 larger than that released by $Z = 0.001$ stars.

Our findings may have important implications for chemical evolution models with dust. In particular, it was sug-

gested that polycyclic aromatic hydrocarbons (PAHs) and carbon dust are mostly produced in AGB stars (Dwek 1998). This has offered an explanation for the observed correlation of PAH line intensities with metallicity in nearby galaxies (Madden et al. 2006). The correlation has been interpreted as a trend of PAH abundance with galactic age, reflecting the delayed injection of PAHs and carbon dust into the ISM by AGB stars in their nal, post-AGB phase of their evolution (Galliano et al. 2008). Our results seem to suggest that the contribution AGB and SAGB to carbon dust enrichment may be significantly less important than previously estimated. The observed correlation may be best attributed to the destruction of PAH molecules by photoevaporation or photodissociation, that are more efficient in low-metallicity environments. A detailed comparison between the yields predicted by the present models and those predicted for massive stars that explode as supernovae (Bianchi & Schneider 2007) is deferred to a future study.

7   CONCLUSIONS

We have calculated the dust formation around intermediate mass stars of metallicity Z=0.008 in the mass range $1 M_{\odot} \leqslant M \leqslant 8 M_{\odot}$ during their whole AGB (or SAGB) phase.

We confirm the main finding of a previous exploration based on a smaller metallicity, i.e. that more massive objects, experiencing HBB, achieve a rich production of sili-

---

[4] The values reported are the same as those shown in Fig. 13 of paper I, where the small extra contribution of silicate dust production at late evolutionary timescales (that is not apparent in Fig.10) is due to a numerical error.
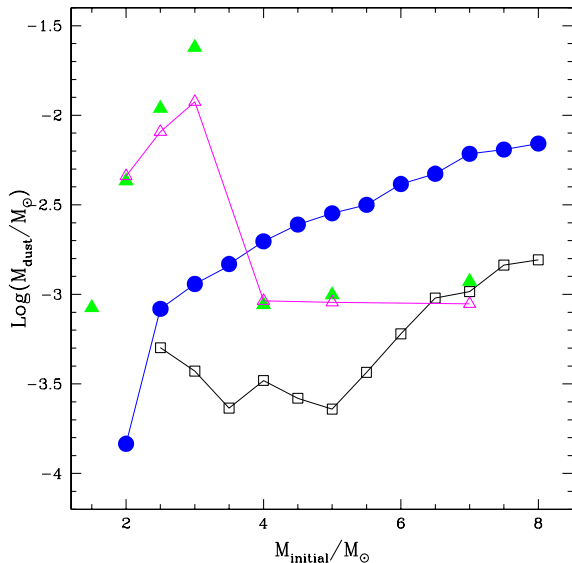
Figure 9. The total mass of dust produced by stars with different initial masses and metallicities. The meaning of the various symbols is the same as in Fig. 8.
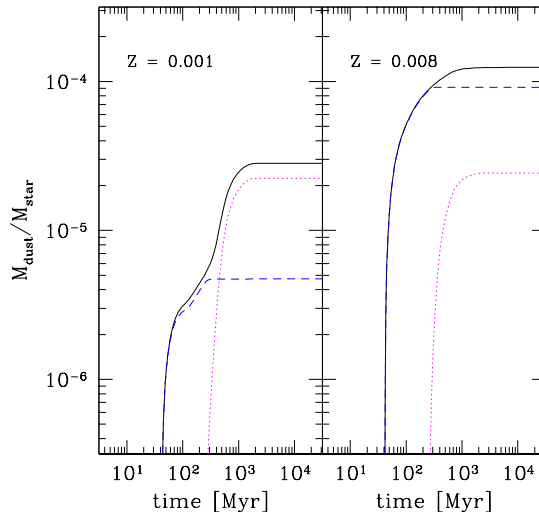

Figure 10. The total mass of dust produced by AGB and SAGB stars normalized to the total mass of stars formed in a single burst at time $= 0$ with a Larson IMF ranging between 1 and $100 M_\odot$ and initial metallicity of $Z = 0.001$ (*left panel*) and of $Z = 0.008$ (*right panel*). The solid lines indicate the total mass of dust, the dotted and dashed lines show the separate contributions of carbon and silicate dust. The stellar evolutionary timescales are computed from the ATON stellar evolutionary model.

cates, favoured by the strong mass loss experienced. Lower–mass stars, on the other hand, after an early phase with a minor production of silicates, will be surrounded by carbon grains, once the surface C/O ratio exceeds unity, as a consequence of repeated TDU episodes.

The amount of silicates produced depends on the metallicity of the stars: compared to the Z=0.001 models analyzed in our previous paper, we expect a much larger dust production here, due both to the larger silicon mass fraction, and to the softer HBB experienced, that prevents total destruction of the water molecules present in the wind, required to produce any kind of silicate.

The major sources of uncertainty in the amount of silicates produced are the treatment of convection, with the relative strength of HBB, and the poor knowledge of the optical constants of the various silicates formed, which reflect into an uncertainty of ~ 0.4dex. On the other hand, under the C–star regime, the most important source of uncertainty in the quantity of carbon dust formed is the extent of the TDU, which is poorly known from first principles: a tiny amount of extra–mixing from the borders of the convective shell developed during the TPs favours a much larger inwards penetration of the convective envelope, and leads to much stronger TDUs; the quantity of dust produced changes dramatically, which confirms the poor robustness of the results obtained in this range of masses.

We also like to point out that the assumed mass-loss rate is (in the present framework) important for the resultant degree of dust condensation as well as the time scale on which the stellar envelope is lost from the star. That, in turn, may affect the dust yield we obtain.

Based on these results, we find that the cosmic dust

yield at this metallicity is higher by a factor ~ 5 compared to the Z=0.001 case discussed in our previous work, and is dominated by silicates at all times. Silicates dominate the cosmic dust yield because of the observed monotonic trend with stellar mass of the total dust mass produced by AGB and SAGB stars. In this scenario, the AGB/SAGB dust production (in which silicates are the favored species produced) dominates over presence of carbon dust grains, the favoured type of dust to be produced by lower-mass stars. This is true even with the larger number of lower-mass stars expected according to any realistic IMF.

ACKNOWLEDGMENTS

REFERENCES

Angulo C., Arnould M., Rayet M., et al., 1999, Nucl.Phys. A, 656, 3

Bell K.R., Lin D.N.C., 1994, ApJ, 427, 987

Bianchi S., Schneider R., 2007, MNRAS, 378, 973

Blöcker T., 1995, A&A, 297, 727

Blöcker T., Schöenberner D., 1991, A&A, 244, L43

Brewster M. Q., 1992, Thermal radiative transfer and properties. John Wiley & Sons, New York

Canuto V.M.C., Mazzitelli I., 1991, ApJ, 370, 295

Cloutman L.D., Eoll J.G., 1976, ApJ, 206, 548

D'Antona F., Mazzitelli T., 1996, ApJ, 470, 1093

Dorschner J., Begemann B., Henning, Th., Jager C., Mutschke H, 1995, A&A, 300, 503

Draine B. T., Lee H. M., 1984, ApJ, 285, 89

Dunne L., Maddox S. J., Ivison R., et al. 2009, MNRAS, 394, 1307

Dwek E., 1998, ApJ, 501, 643

Ferrarotti A.D., Gail H.P., 2001, A&A, 371, 133

Ferrarotti A.D., Gail H.P., 2002, A&A, 382, 256

Ferrarotti A.D., Gail H.P., 2006, A&A, 553, 576

Formicola A., Imbriani G., Costantini H., et al., 2004, Phys. Lett. B, 591, 61

Fynbo H.O.U., et al, 2005, Nature, 433, 136

Gail H.P., Sedlmayr E., 1985, A&A, 148, 183

Gail H.P., Sedlmayr E., 1999, A&A, 347, 594

Gallerani S., Maiolino R., Juarez Y., et al., 2010, A&A, 523, A85

Galliano F., Dwek E., Chanial P., 2008, ApJ, 672, 214

Garcia-Berro E., Ritossa C., Iben I.J., 1997, ApJ, 485, 765

Gil-Pons P., Gutierrez J., Garcia-Berro E., 2007, A&A, 464, 667

Grevesse N., Sauval A.J, 1998, SSrv, 85, 161

Groenewegen M. A. T.., de Jong T., 1993, A&A, 267, 410

Herwig F., 2000, A&A, 360, 952

Herwig F., 2005, AR&A, 43, 435

Herwig F., Austin S.M., 2004, ApJ, 613, L73

Hirashita H., Nozawa T., Takeuchi T. T., Kozasa T., 2008, MNRAS, 384, 1725

Höfner S., 2008, A&A, 491, L1

Iben I. Jr., 1975, ApJ, 196, 525

Iben I. Jr., 1976, ApJ, 208, 165

Iglesias C. A., Rogers F. J., 1996, ApJ, 464, 943

Izzard R. G., Tout C. A., Karakas A. I., Pols O. R., 2004, MNRAS, 350, 407

Jager C., Mutschke H., Begemann B., Dorschner J., Henning Th., 1994, A&A, 292, 641

Jeong K. S., Winters J. M., Le Bertre T., Sedlmayr E., 2003, A&A, 407, 191

Jones T. W., Merrill K. M., 1976, ApJ, 509, 524

Karakas A.I., 2011, in ASP Conf. Ser., Why Galaxies Care about AGB Stars II: Shining Examples and Common Inhabitants. Proceedings of a conference held at University Campus, Viena, Austria, 16-20 August 2010. Edited by F. Kerschbaum, T. Lebzelter, and R.F. Wing. San Francisco: Astronomical Society of the Pacific, 2011., 455, p.3

Karakas A. I., Campbell S. W., Stancliffe R. J., 2010, ApJ, 713, 374

Knapp G. R., 1985, ApJ, 293, 273

Kunz R., Fey M., Jaeger M., Mayer A., Hammer J.W., Staudt G., Harissopulos S., Paradellis T., 2002, ApJ, 567, 643

Lattanzio J. C., 1986, ApJ, 311, 708

Lattanzio J. C., 1989, ApJ, 344, L25

Lucy L.B., 1976, ApJ, 205, 482

Madden S. C., Galliano F., Jones, A. P., Sauvage M., 2006, A&A, 446, 877

Maiolino R., Schneider R., Oliva E., et al. 2004, Nature, 431, 533

Marigo P., 2002, A&A, 387, 507

Marigo P., Girardi L., Bressan A., 1999, A&A, 344, 123

Marigo P., Aringer B., 2009, A&A, 508, 1538

Mattsson L., Höfner S., 2011, A&A, 533, A42

Morgan H. L., Dunne L., Eales S. A., Ivison R. J., Edmunds M. G., 2003, ApJ, 597, L33

Mowlavi N., 1999, A&A, 344, 617

Norris B. R. M., Tuthill P. G., Ireland M. J., et al., 2012, Nature, 484, 220

Ossenkopf V., Henning Th., Mathis J. S., 1992, A&A, 261, 567

Renzini A., Voli M., 1981, A&A, 94, 175

Rho J., Kozasa T., Reach W. T., et al. 2008, ApJ, 673, 271

Schwarzschild M., Harm R., 1965, ApJ, 142, 855

Schwarzschild M., Harm R., 1967, A&A, 145, 486

Siess L., 2007, A&A, 476, 893

Siess L., 2010, A&A, 512, A10

Stancliffe R. J., Izzard R. G.,Tout C. A., 2005, MNRAS, 356, L1

Stancliffe R. J.,Tout C. A., Pols, O. R., 2004, MNRAS, 352, 984

Straniero O., Chieffi A., Limongi M., Busso M., Gallino R., Arlandini, C., 1997, ApJ, 478, 332

Stratta G., Gallerani S., Maiolino R., 2011, A&A, 532, 45

Todini P., Ferrara A., 2001, MNRAS, 325, 726

Valiante R., Schneider R., Bianchi S., Andersen A., Anja C., 2009, MNRAS, 397, 1661

Valiante R., Schneider R., Salvadori S., Bianchi S., 2011, MNRAS, 416, 1916

Vassiliadis E., Wood P.R., 1993, ApJ, 413, 641

Ventura P., Carini R., D'Antona F., 2011, MNRAS, 415, 3865

Ventura P., D'Antona F., 2005a, A&A, 341, 279

Ventura P., D'Antona F., 2009, A&A, 499, 835

Ventura P., D'Antona F., 2011, MNRAS, 410, 2760

Ventura P., D'Antona F., Mazzitelli I., 1999, ApJ, 524, L11

Ventura P., D'Antona F., Mazzitelli I., 2000, A&A, 363, 605

Ventura P., Di Criscienzo M., Schneider R., Carini R., Valiante R., D'Antona F., Gallerani S., Maiolino R., Tornambé A., 2012, MNRAS, 420, 1442

Ventura P., Marigo P., 2009, MNRAS, 399, L54

Ventura P., Marigo P., 2010, MNRAS, 408, 2476

Ventura P., D'Antona F., Mazzitelli I., 2000, A&A, 363, 605

Ventura P., Zeppieri A., Mazzitelli I., D'Antona F., 1998, A&A, 334, 953

Wachter A., Winters J. M., Schroeder K. P:, Sedlmayr E., 2008, A&A, 497, 504

Wood P. R., 1981, In Physical processes in Red Giants, ed. I: Iben Jr., A. Renzini, p. 135. Dordrecht, The Netherlands: Reidel

Zhukovska S., Gail H. P., Trieloff M., 2008, A&A, 479, 453

Zhukovska S., Gail H. P., 2009, *Cosminc Dust – near and far* ASP Conference Series, 2009, 414, 199. Th. Enning, E. Grun and J. Steinacker eds.